On Causes for Solution Inconsistencies and their Localization by Means of a Generic Finite-Element Multi-Field Approach Applied to Semiconductor Simulation

***Abstract* — A local assessment of solution stability of highly non-linear coupled multi-field partial differential equations discretized by the finite element method is presented. The assessment is based on a set of generic multi-physical partial differential equations, which is exemplary applied to the drift-diffusion semiconductor carrier transport model. The semiconductor problem, as the standard model for semiconductor device simulation, renders a coupled non-linear system of equations. The system is known for causing convergence problems in the iterative non-linear solution procedure. The solution process strongly depends on the discretization. We investigate the influence of physical parameters on the convergence by applying two general instability indicators, the Péclet and the Damköhler number, to the Jacobian of the discrete semiconductor problem. The use of analytic or symbolic derivatives of physical parameters provides the sought insight to the causes of instabilities.**

I. Introduction

It is known from finite element analysis of elliptic partial differential equations (PDEs) that co-occurrence of convection and reaction with diffusion may cause the classical Galerkin method to produce solution inconsistencies on coarse discretizations. This is particularly true if convection or reaction become dominant compared to diffusion. Characteristic numbers stemming from ratios of reaction or convection over diffusion considering the mesh size indicate the occurrence of solution inconsistencies [1, 2]. A prominent example of such a figure is the mesh Péclet number. It quantifies the ratio between convective and diffusive flows with regard of the mesh size. If the mesh Péclet number is large the problem becomes singularly perturbed and sharp boundary layers appear that cannot be resolved by the mesh. In this case, the simulation results show heavy, spurious, non-physical oscillations which may extend over broad regions.

While it is common to employ *h*- or *hp*-(self-)adaptation methods to resolve problems related to coarse meshing, this approach may not be feasible for convection-dominated problems. The solution on a coarse mesh often does not show the characteristics of the true solution and often is non-physical. A remedy is found in stabilization methods such as SUPG (also termed as SDFEM) or the Scharfetter-Gummel method [3, 4]. These methods are deduced from linear one-dimensional considerations on an equidistant mesh whereas generalizations to the multi-dimensional, multi-physical and non-linear cases on graded meshes are a continuing research topic.

For the class of diffusion-convection-reaction problems, a further parameter exists that quantifies the ratio between the diffusion and reaction. Such a parameter has been used e. g. by Idelsohn and Hernandez [5, 2]. We refer to that parameter as the Damköhler number. The majority of publications concentrate on instabilities caused by high Péclet number and comparably fewer consider the combined effect with high Damköhler number [6, 7].

Convection-diffusion problems appear in various technical areas such as electrochemistry, fluid flow problems, chemical reactor design, magnetohydrodynamics and motional induction, to name few. As an interesting example we investigate the problem of charge transport in semiconductors.

The classical finite-element drift-diffusion semiconductor problem is based on Boltzmann transport equation. It has been successfully employed in one spatial dimension by Gummel [8] and has been extended to a two-dimensional finite-difference calculation by Slotboom [9]. Since then much progress has been achieved on the subject of modeling the semiconductor current transport by means of the finite element method to various aspects of the modeling difficulties [10, 11].

For a long period of time and even until today, the two-dimensional simulation of the semiconductor devices is still in use. Despite the growth of computational power, simulation of semiconductor carrier transport in three dimensions remains limited to small spatial regions or basic electronic components such as single transistors or diodes. That is due to extensive requirements on the mesh density that are imposed by the model to produce physically consistent solutions. Furthermore, the drift-diffusion semiconductor model is highly non-linear. Therefore, the problem must be solved by an iterative solver, ideally a Newton iteration, employing a full Jacobian matrix re-computed in each iteration step, which makes the solution of semiconductor charge transport computationally expensive.

Obtaining a convergent simulation is often a trial and error process. There is always the attempt to obtain a meaningful solution by means of as little computational effort as possible. Making the mesh size smaller in necessary regions and leaving it tolerable coarse elsewhere is an often employed strategy - but how to decide where to set the regions of small mesh size? Analytic considerations suggest the use of a mesh size close to the charge carriers Debye length. That requirement proposes element size in order of nanometres, which makes the vast majority of practical semiconductor device simulations not feasible by means of reasonable computational expense.

Locating regions with insufficiently fine mesh size is not a straightforward task. There are some well-known spots in a model tending to produce solution failures such as regions in vicinity to contacts or boundaries with Dirichlet boundary conditions and the regions with high net doping gradient. Locating regions in the model that cause instabilities by means of the Péclet and the Damköhler numbers can be beneficial and a more straightforward approach.

By means of a generic model for second-order partial differential equations, we aim to apply a technique for indication of solution inconsistency to the semiconductor problem which can also be generalized to other multi-physical applications. Generally speaking, all models that are formulated as partial differential equations of second order are seen as consisting of distinct generic terms: diffusion, convection and reaction.

The mapping of parameters of a specific problem such as for example the semiconductor drift-diffusion model must be done by choosing coefficients of distinct terms of the generic model (4) to replicate the problem statement. For the drift-diffusion semiconductor model that mapping is presented in section III. At

first glance it may seem that the model comprises of diffusion and convection terms only. At a further analysis of the Jacobian, it is found that the model includes diffusion, convection and reaction simultaneously.

II. The physical model and finite-element equations

The multi-physical problem is established by means of a generic partial differential equation given by r in (1). In a multi-physics setting, r is a vectorial function

$$r^s\left(u^t\right) = 0. \tag{1}$$

The generic formulation of a multi-physical equation over the domain Ω is given in the differential form by equation (2). Equation (3) presents the general boundary condition to hold on $\partial\Omega$.

$$r^s = -\frac{\partial}{\partial x_i}\left(\nu_{ij}^{st}\frac{\partial u^t}{\partial x_j} + \gamma_i^{st}u^t + g_i^s\right) + \beta_j^{st}\frac{\partial u^t}{\partial x_j} + \alpha^{st}u^t - f^s \quad \text{in } \Omega \tag{2}$$

$$n_i\left(\nu_{ij}^{st}\frac{\partial u^t}{\partial x_j} + \gamma_i^{st}u^t + g_i^s\right) = q^{st}u^t + p^s \quad \text{on } \partial\Omega \tag{3}$$

To reach notational brevity we use sum convention (Einstein notation) which implies summation over co-occurrent indices in each term. Indices s, t enumerate scalar fields, indices i, j enumerate spatial coordinates and indexes n, m will denote degrees of freedom in the following. Each index is interchangeable by other index of the same group without altering the meaning. Table I presents the index symbols, their ranges and the corresponding variables. The total number of simultaneously considered scalar fields is n_{sf}, whereas n_{dof} denotes the total number of degrees of freedom.

Without loss of generality, indices may range either over the whole discretized domain or over subsets, such as a single element or a compound of elements. Field-denoting indices are placed in superscript exclusively, making it easy to obtain a single-field representation of given equations by dropping field-enumerating superscripts.

Equation (2) incorporates the coefficients ν_{ij}^{st}, γ_i^{st}, β_j^{st} and α^{st} which in most engineering and physical problems are identified as material properties. Spatial indices i, j indicate that material properties are assumed to be anisotropic. An overview of all terms of the generic PDE is given in Table II.

Given that ξ_n^t are the shape functions and ξ_m^s are the test functions and setting

$$u^t = w_n\xi_n^t$$

the weak form of the generic multi-field equation is written as follows:

Table I. Indices used in the sum convention

Group	Corresponding Variables	Reserved Symbols	Range
spatial coordinates	x_i, x_j	i, j, l	$1...n_{\text{dim}}$
degrees of freedom	w_m, w_n, w_p	m, n, p	$1...n_{\text{dof}}$
scalar fields	u^s, u^t, u^v	s, t, v	$1...n_{\text{sf}}$

$$\begin{aligned} r_m = &\int_\Omega\left(\nu_{ij}^{st}\frac{\partial\xi_n^t}{\partial x_j} + \gamma_i^{st}\xi_n^t\right)\frac{\partial\xi_m^s}{\partial x_i}\cdot w_n \\ &+\int_\Omega\left(\beta_j^{st}\frac{\partial\xi_n^t}{\partial x_j} + \alpha^{st}\xi_n^t\right)\xi_m^s\cdot w_n \\ &-\int_{\partial\Omega} q^{st}\xi_n^t\xi_m^s\cdot w_n \\ &+\int_\Omega g_i^s\frac{\partial\xi_m^s}{\partial x_i} - \int_\Omega f^s\xi_m^s - \int_{\partial\Omega} p^s\xi_m^s \end{aligned} \tag{4}$$

By mapping of material properties to coefficients of (4) the global system of coupled multi-physical equations is established for each specific physical equation:

$$r_m = A_{mn}w_n - b_m \tag{5}$$

In a non-linear setting $\nu_{ij}^{st}(u^t)$, $\gamma_i^{st}(u^t)$, $\beta_j^{st}(u^t)$, $\alpha^{st}(u^t)$, $f^s(u^t)$ and $g_i^s(u^t)$ are functions of the unknowns. In that case, the solution is obtained in an iterative process by subsequently applying

$$w_n^* = w_n + \delta w_n \tag{6}$$

from a series of intermediate solution steps δw_n starting from w_n and stepping towards a better estimate of the final solution w_n^*. The steps are computed by means of an iteration matrix. By each iteration step the final solution is approached except for cases where the iteration leads to divergence.

If the iteration matrix is chosen to be the Jacobian J_{mn}, we refer to iteration (6) as Newton iteration which is preferred according to its high convergence rate. The Jacobian is constructed from n derivatives of the residual vector r_m with respect to the degrees of freedom:

$$J_{mn} = \frac{\partial r_m\left(w_p\right)}{\partial w_n} \tag{7}$$

The global system of equations rearranged in the non-linear setting becomes

$$J_{mn}\delta w_n = -r_m \tag{8}$$

or written out as a set of intermediate terms by using (5) and (7)

$$\left[A_{mn} + \frac{\partial A_{mp}}{\partial w_n}w_p - \frac{\partial b_m}{\partial w_n}\right]\delta w_n = -\left(A_{mp}w_p - b_m\right) \tag{9}$$

Here we use the index p as subsidiary of n to avoid notational ambiguity.

In the global system of non-linear equations we find the terms A_{mn} and b_m which are obtained by a single evaluation of r_m. The rest of the Jacobian terms are established by means of derivatives which presents a more laborious task. We refer to

Table II. PDE terms for the generic equation

Term	Mathematical Formulation	Physical Meaning
ν-term	$\nabla\cdot\left(\nu_{ij}^{st}\nabla\left(u^t\right)\right) = \frac{\partial}{\partial x_i}\left(\nu_{ij}^{st}\frac{\partial u^t}{\partial x_j}\right)$	Diffusion
γ-term	$\nabla\cdot\left(\gamma_i^{st}u^t\right) = \frac{\partial}{\partial x_i}\left(\gamma_i^{st}u^t\right)$	Convection
β-term	$\beta_j^{st}\nabla u^t = \beta_j^{st}\frac{\partial u^t}{\partial x_j}$	Convection
α-term	$\alpha^{st}u^t$	Reaction
f-term	f^s	Field source
g-term	$\nabla\cdot\left(g_i^s\right) = \frac{\partial}{\partial x_i}g_i^s$	Flux source

A_{mn} and b_m as residual terms whereas $\frac{\partial A_{mp}}{\partial w_n} w_p$ and $\frac{\partial b_m}{\partial w_n}$ are called the Jacobian terms.

Before addressing the calculation of the Jacobian terms, the semiconductor drift-diffusion problem is derived in terms of the generic equations (4) and (9) in the following section.

III. Semiconductor drift-diffusion model

The semiconductor drift-diffusion model consists of three partial differential equations. The Poisson equation describes the electrical potential depending on the space charge distribution. Two drift-diffusion equations for electrons n and holes p govern the semiconductor charge transport. The thermal effects on the device characteristics (e.g. charge carrier mobilities) are considered negligible in the given setup.

$$\nabla \cdot E = \nabla \cdot (-\nabla \Psi) = \rho \tag{10}$$

$$\nabla \cdot J_\mathrm{n} = \nabla \cdot \left[q_\mathrm{e} \mu_\mathrm{n} \left(n \nabla \Psi + V_\mathrm{th} \nabla n \right) \right] = q_\mathrm{e} R_\mathrm{SRH} \tag{11}$$

$$\nabla \cdot J_\mathrm{p} = \nabla \cdot \left[q_\mathrm{e} \mu_\mathrm{p} \left(p \nabla \Psi - V_\mathrm{th} \nabla p \right) \right] = -q_\mathrm{e} R_\mathrm{SRH} \tag{12}$$

$$R_\mathrm{SRH} = \frac{np - n_\mathrm{i}^2}{\tau_\mathrm{n} \left(p + p_0 \right) + \tau_\mathrm{p} \left(n + n_0 \right)} \tag{13}$$

Equation (4) models the Poisson equation (10) if the electric potential represents the unknown and the ν_{ij}^{st}-term is the permittivity tensor of the material. The right-hand side sums up the total charge carrier concentrations by means of the f^s-term. In that way, the drift-diffusion carrier transport equations (11), (12) are both coupled to the Poisson equation trough the source term $f^{s=1}$.

There is a certain freedom how individual terms are mapped to those of the generic equation. For instance, the charge carrier concentrations n, p can also be represented by setting $\alpha^{st}|_{s=1,t=2,3} = 1$. We will see later that considering the Jacobian both ways of coupling will result in the same final matrix.

The three potentials u_1, u_2, u_3 for the semiconductor problem represent the three scalar fields: electric potential Ψ, electron n and hole p carrier concentrations.

The basic semiconductor equations provided in form of generic terms read as follows:

$$r^1 = -\frac{\partial}{\partial x_i} \left(\epsilon_{ij} \frac{\partial \Psi}{\partial x_j} \right) - q_\mathrm{e} \left(p - n + N_\mathrm{D} - N_\mathrm{A} \right) \tag{14}$$

$$r^2 = -\frac{\partial}{\partial x_i} \left(D_{\mathrm{n}ij} \frac{\partial n}{\partial x_j} - \mu_\mathrm{n} \frac{\partial \Psi}{\partial x_i} n \right) + R_\mathrm{SRH} \tag{15}$$

$$r^3 = -\frac{\partial}{\partial x_i} \left(D_{\mathrm{p}ij} \frac{\partial p}{\partial x_j} + \mu_\mathrm{p} \frac{\partial \Psi}{\partial x_i} p \right) + R_\mathrm{SRH} \tag{16}$$

Equations (14) - (16) present the full set of residual terms, from which the Jacobian terms must be derived. We will see that the Jacobian terms are of the same form as A_{mn}. The resulting Jacobian terms form an additive matrix component that we refer to as the Jacobian component Φ_{mn} which contains only the Jacobian terms (terms stemming from derivatives of A_{mn}). The sum of the two by means of (7) yields the general Jacobian matrix:

$$\begin{aligned} J_{mn} &= \frac{\partial}{\partial w_n} \left(A_{mp} w_p - b_m \right) \\ &= A_{mn} + \frac{\partial A_{mp}}{\partial w_n} w_p - \frac{\partial b_m}{\partial w_n} = A_{mn} + \Phi_{mn} \end{aligned} \tag{17}$$

There are different ways in which derivatives are typically obtained in a practical implementation, i. e. by numerical differentiation or automatic differentiation. We consider analytical derivatives, which enables us to reveal important numerical implications of the distinct Jacobian terms. When assembling the Jacobian, the sum of Jacobian and residual terms

Table III. Physical parameters of the semiconductor problem

Parameter	Intrinsic Relation	Simulation default value	Unit	Description
x			m	Spatial variable
q_e		$1.602 \cdot 10^{-19}$	As	Electron charge
T		300	K	Temperature
Ψ			V	Electrical potential
V_bi	$V_\mathrm{bi} = \frac{k_\mathrm{B} T}{q_\mathrm{e}} \ln \left(\frac{N_\mathrm{A} N_\mathrm{D}}{n_\mathrm{i}^2} \right)$		V	Build-in voltage
V_th	$V_\mathrm{th} = \frac{k_\mathrm{B} T}{q_\mathrm{e}}$		V	Thermal voltage
ϵ	$\epsilon_r \epsilon_0$	$\epsilon_r = 11.9$	$\frac{\mathrm{As}}{\mathrm{Vm}}$	Dielectric constant
n	$n = n_\mathrm{i} \mathrm{e}^{\frac{\Psi - \Phi_\mathrm{n}}{V_\mathrm{th}}}$		$\frac{1}{\mathrm{m}^3}$	Electrons density
p	$p = n_\mathrm{i} \mathrm{e}^{\frac{\Phi_\mathrm{p} - \Psi}{V_\mathrm{th}}}$		$\frac{1}{\mathrm{m}^3}$	Holes density
n_i	$np = n_\mathrm{i}^2$	10^{16}	$\frac{1}{\mathrm{m}^3}$	Intrinsic carrier concentration
N_A		$N_{\mathrm{A}_0} = 10^{22}$	$\frac{1}{\mathrm{m}^3}$	Acceptor doping concentration
N_D		$N_{\mathrm{D}_0} = 10^{19}$	$\frac{1}{\mathrm{m}^3}$	Donator doping concentration
μ_n		0.14	$\frac{\mathrm{m}^2}{\mathrm{Vs}}$	Electron mobility
μ_p		0.045	$\frac{\mathrm{m}^2}{\mathrm{Vs}}$	Hole mobility
D_n	$D_\mathrm{n} = \mu_\mathrm{n} V_\mathrm{th}$		$\frac{\mathrm{m}^2}{\mathrm{s}}$	Electron diffusivity
D_p	$D_\mathrm{p} = \mu_\mathrm{p} V_\mathrm{th}$		$\frac{\mathrm{m}^2}{\mathrm{s}}$	Hole diffusivity
R_SRH	$R_\mathrm{SRH} = \frac{np - n_\mathrm{i}^2}{\tau_\mathrm{n}\left(p + p_0\right) + \tau_\mathrm{p}\left(n + n_0\right)}$		$\frac{1}{\mathrm{sm}^3}$	Shockley-Read-Hall recombination
τ_n	$\tau_\mathrm{n} = \frac{\tau_{\mathrm{n}0}}{1 + \frac{N_\mathrm{D} + N_\mathrm{A}}{n_\mathrm{i}}}$	$3.95 \cdot 10^{-5}$	s	Electron lifetime
τ_p	$\tau_\mathrm{p} = \frac{\tau_{\mathrm{p}0}}{1 + \frac{N_\mathrm{D} + N_\mathrm{A}}{n_\mathrm{i}}}$	$3.52 \cdot 10^{-6}$	s	Hole lifetime

$A_{mn} + \Phi_{mn}$ may cause the overall non-linear problem to become of diffusion-convection-reaction type. In that case it may be shown that material parameters can negatively affect the stability of the Newton iteration.

In all practical cases of non-linear multi-physical problems the material parameters depend on the potentials u^t or their gradients $\mathcal{G}_l^v = \frac{\partial u^v}{\partial x_l}$. In the case of the drift-diffusion model those are Ψ, n, p and $\nabla\Psi$, ∇n, ∇p respectively.

The derivatives in a general setting are given by:

$$\begin{aligned}\Phi_{mn}\left(u^t\right) = &\int_\Omega \left(\frac{\partial \nu_{ij}^{st}}{\partial u^v}\frac{\partial u^t}{\partial x_j} + \frac{\partial \gamma_i^{st}}{\partial u^v}u^t + \frac{\partial g_i^s}{\partial u^v}\right)\xi_n^v\frac{\partial \xi_m^s}{\partial x_i}\\ &+\int_\Omega \left(\frac{\partial \beta_j^{st}}{\partial u^v}\frac{\partial u^t}{\partial x_j} + \frac{\partial \alpha^{st}}{\partial u^v}u^t - \frac{\partial f^s}{\partial u^v}\right)\xi_n^v\xi_m^s\\ &-\int_{\partial\Omega}\left(\frac{\partial q^{st}}{\partial u^v}u^t + \frac{\partial p^s}{\partial u^v}\right)\xi_n^v\xi_m^s\\ &=\int_\Omega \mathring{\gamma}_i^{sv}\xi_n^v\frac{\partial \xi_m^s}{\partial x_i} + \mathring{\alpha}^{sv}\xi_n^v\xi_m^s - \int_{\partial\Omega}\breve{\alpha}^{sv}\xi_n^v\xi_m^s\end{aligned}$$

$$\begin{aligned}\Phi_{mn}\left(\mathcal{G}_l^v\right) = &\int_\Omega \left(\frac{\partial \nu_{ij}^{st}}{\partial \mathcal{G}_l^v}\frac{\partial u^t}{\partial x_j} + \frac{\partial \gamma_i^{st}}{\partial \mathcal{G}_l^v}u^t + \frac{\partial g_i^s}{\partial \mathcal{G}_l^v}\right)\frac{\partial \xi_n^v}{\partial x_l}\frac{\partial \xi_m^s}{\partial x_i}\\ &+\int_\Omega \left(\frac{\partial \beta_j^{st}}{\partial \mathcal{G}_l^v}\frac{\partial u^t}{\partial x_j} + \frac{\partial \alpha^{st}}{\partial \mathcal{G}_l^v}u^t - \frac{\partial f^s}{\partial \mathcal{G}_l^v}\right)\frac{\partial \xi_n^v}{\partial x_l}\xi_m^s\\ &-\int_{\partial\Omega}\left(\frac{\partial q^{st}}{\partial \mathcal{G}_l^v}u^t + \frac{\partial p^s}{\partial \mathcal{G}_l^v}\right)\frac{\partial \xi_n^v}{\partial x_l}\xi_m^s\\ &=\int_\Omega \mathring{\nu}_{il}^{sv}\frac{\partial \xi_n^v}{\partial x_l}\frac{\partial \xi_m^s}{\partial x_i} + \mathring{\beta}_l^{sv}\frac{\partial \xi_n^v}{\partial x_l}\xi_m^s - \int_{\partial\Omega}\breve{\beta}_l^{sv}\frac{\partial \xi_n^v}{\partial x_l}\xi_m^s\end{aligned}$$

An analysis of the above Jacobian terms shows that the derivatives of $\nu_{ij}^{st}\left(u^t\right)$, $\gamma_i^{st}\left(u^t\right)$ and $g_j^{st}\left(u^t\right)$ in the residuum equation (4) with respect to the unknown add a $\mathring{\gamma}_i$ term to the Jacobian.

The derivatives of $\beta_j^{st}\left(u^t\right)$, $\alpha^{st}\left(u^t\right)$ and $f^s\left(u^t\right)$ with respect to the unknown add a $\mathring{\alpha}$ terms to the global Jacobian. In analogy, when differentiated with respect to the gradient of the unknown, additional $\mathring{\nu}_{ij}$ and $\mathring{\beta}_j$ terms are introduced.

Of special interest for the semiconductor problem are two cases: The first case results from the non-linear ν_{ij}-term of the electrons and holes transport equations (the drift current component). When differentiated with respect to the unknowns, it contributes $\mathring{\gamma}_i = \mu_{\mathrm{n,p}}\frac{\partial\Psi}{\partial x_i}$ in proportion to the gradient of the electric potential, in other words the electric field. In the second case, differentiation of f-terms of the carrier transport equations representing the carrier recombination rate add $\mathring{\alpha} = \frac{\partial R_{SRH}}{\partial n}$ or $\mathring{\alpha} = \frac{\partial R_{SRH}}{\partial p}$.

Considering the terms occurring in the Jacobian according to (17) in combination with expressions for $\Phi_{mn}\left(u^t\right)$ it is irrelevant whether n and p are placed on the right-hand side of the Poisson equation or as α^{st}-terms. In either case, the Jacobian consists of $\alpha^{st} + \mathring{\alpha}^{st}$ which leads to the same final expression. A similar situation appears for the (non-linear) drift current and the product of electric field strength and carrier concentration which either could be interpreted as a γ- or a ν-term. That way, in the context of the Newton iteration, the non-linear semiconductor drift-diffusion model in fact is a diffusion-convection-reaction type of problem, which is prominent for being unstable and it is not possible to rearrange terms such that the unfavorable numerical properties disappear.

Differentiation of r^1, r^2 and r^3 yields the Jacobian terms provided in the following:

$$\Phi_{11} = \frac{\partial r^1}{\partial\nabla\Psi} = -\frac{\partial}{\partial x_i}\left(\epsilon_i\right) = 0 \tag{18}$$

$$\Phi_{12} = \frac{\partial r^1}{\partial n} = q_{\mathrm{e}} \tag{19}$$

$$\Phi_{13} = \frac{\partial r^1}{\partial p} = -q_{\mathrm{e}} \tag{20}$$

$$\Phi_{21} = \frac{\partial r^2}{\partial\nabla\Psi} = \nabla\cdot\left(\mu_{\mathrm{n}}n\right) \tag{21}$$

$$\Phi_{22} = \frac{\partial r^2}{\partial n} + \frac{\partial r^2}{\partial\nabla n} = \frac{\partial R_{\mathrm{SRH}}}{\partial n} + \nabla\cdot\left(D_{\mathrm{n}}\right) \tag{22}$$

$$\Phi_{23} = \frac{\partial r^2}{\partial p} + \frac{\partial r^2}{\partial\nabla p} = \frac{\partial R_{\mathrm{SRH}}}{\partial p} \tag{23}$$

$$\Phi_{31} = \frac{\partial r^3}{\partial\nabla\Psi} = \nabla\cdot\left(\mu_{\mathrm{p}}p\right) \tag{24}$$

$$\Phi_{32} = \frac{\partial r^3}{\partial n} = \frac{\partial R_{\mathrm{SRH}}}{\partial n} \tag{25}$$

$$\Phi_{33} = \frac{\partial r^3}{\partial p} = \frac{\partial R_{\mathrm{SRH}}}{\partial p} \tag{26}$$

with

$$\frac{\partial R_{\mathrm{SRH}}}{\partial n} = \frac{p\left(\tau_{\mathrm{n}}\left(p+p_0\right)+\tau_{\mathrm{p}}\left(n+n_0\right)\right)-\tau_{\mathrm{p}}\left(np-n_{\mathrm{i}}^2\right)}{\left(\tau_{\mathrm{n}}\left(p+p_0\right)+\tau_{\mathrm{p}}\left(n+n_0\right)\right)^2} \tag{27}$$

$$\frac{\partial R_{\mathrm{SRH}}}{\partial p} = \frac{n\left(\tau_{\mathrm{n}}\left(p+p_0\right)+\tau_{\mathrm{p}}\left(n+n_0\right)\right)-\tau_{\mathrm{n}}\left(np-n_{\mathrm{i}}^2\right)}{\left(\tau_{\mathrm{n}}\left(p+p_0\right)+\tau_{\mathrm{p}}\left(n+n_0\right)\right)^2} \tag{28}$$

$$\begin{bmatrix}\begin{bmatrix}\nu_{ij}^{11}=\epsilon_{ij}\end{bmatrix} & \begin{bmatrix}\mathring{\alpha}^{12}=q_{\mathrm{e}}\end{bmatrix} & \begin{bmatrix}\mathring{\alpha}^{13}=-q_{\mathrm{e}}\end{bmatrix}\\ \begin{bmatrix}\nu_{ij}^{21}=-\mu_{\mathrm{n}}n\end{bmatrix} & \begin{bmatrix}\nu_{ij}^{22}=D_{\mathrm{n}}\\ \mathring{\gamma}_i^{22}=-\mu_{\mathrm{n}}\nabla\Psi\\ \mathring{\alpha}^{22}=\frac{\partial R_{\mathrm{SRH}}}{\partial n}\end{bmatrix} & \begin{bmatrix}\mathring{\alpha}^{23}=\frac{\partial R_{\mathrm{SRH}}}{\partial p}\end{bmatrix}\\ \begin{bmatrix}\nu_{ij}^{31}=\mu_{\mathrm{p}}n\end{bmatrix} & \begin{bmatrix}\mathring{\alpha}^{32}=\frac{\partial R_{\mathrm{SRH}}}{\partial n}\end{bmatrix} & \begin{bmatrix}\nu_{ij}^{33}=D_{\mathrm{p}}\\ \mathring{\gamma}_i^{33}=\mu_{\mathrm{p}}\nabla\Psi\\ \mathring{\alpha}^{33}=\frac{\partial R_{\mathrm{SRH}}}{\partial p}\end{bmatrix}\end{bmatrix}\begin{bmatrix}\Psi\\ n\\ p\end{bmatrix} = \begin{bmatrix}f^1=q_{\mathrm{e}}\cdot\left(N_{\mathrm{D}}+p-N_{\mathrm{A}}-n\right)\\ f^2=-R_{\mathrm{SRH}}\\ f^3=-R_{\mathrm{SRH}}\end{bmatrix}$$

IV. Comparison of discrete and continuous equations

The arrangement of coefficients as given above helps in analyzing the instabilities in the semiconductor problem. According to the above proposition, the type of the term of a coefficient as well as the magnitude of the parameters are crucial for the stability of the Newton iteration. It may not be an obvious observation that the problems arise not from the underlining equation system, but rather from the Galerkin-discretized model of the problem.

In order to elucidate and analyze the primary cause of instabilities we consider the simplified case of the one-dimensional version of the continuous (2) and the discrete counterpart (4). The continuous problem has a solution which has the form

$$u\left(x\right) = a_1 e^{\lambda_1 x} + a_2 e^{\lambda_2 x} \tag{29}$$

with λ_1 and λ_2 being the roots of the characteristic polynomial of the 1D differential equation (assuming β incorporates both convection terms)

$$\lambda_{1,2} = \frac{\beta \pm \sqrt{\beta^2 + 4\alpha\nu}}{2\nu} \tag{30}$$

Assuming u_1, u_2, u_3 denoting the discrete potential values at three neighboring grid points and h being the mesh size, the Galerkin discretization produces a discrete stencil:

$$\left(-\nu + \beta\frac{h}{2} + \alpha\frac{h^2}{6}\right) u_3 + \left(2\nu + \alpha\frac{2h^2}{3}\right) u_2 + \left(-\nu - \beta\frac{h}{2} + \alpha\frac{h^2}{6}\right) u_1 = 0 \tag{31}$$

The discrete difference equation has the solution:

$$u_k = a_1\mu_1^k + a_2\mu_2^k \tag{32}$$

The roots μ_1, μ_2 of the characteristic polynomial for the discrete solution are given by

$$\mu_{1,2} = \frac{2 + \frac{2}{3}\alpha h^2 \pm h\sqrt{\beta^2 + 4\nu\alpha + \frac{1}{3}\alpha^2 h^2}}{2\nu - \beta h - \frac{1}{3}\alpha h^2} \tag{33}$$

Therefore, the roots of the discrete characteristic polynomial inherit the dependence on the mesh size. The continuous problem shows oscillatory behavior only for $\beta^2 + 4\alpha\nu$, while the discrete counterpart also exhibits oscillatory behavior if the roots $\mu_{1,2}$ are negative (odd and even exponentials cause u_k of neighboring mesh nodes to flip the sign, see (32)). This behavior is nonconforming to that of the continuous solution, i. e. the oscillations are spurious.

From equation (33), a condition indicating if a transition of the roots to the negative region occurs depending on α, β-parameters in combination with the local mesh size may be deduced:

$$2\nu - |\beta|h - \frac{1}{3}\alpha h^2 > 0 \tag{34}$$

Specifically, the diffusion coefficient ν may become small in comparison with the combination of convection β and the reaction α coefficients and mesh size. The mesh Péclet number Pe, which is the ratio between diffusive and convective flows over a characteristic length provides one measure to assess that performance insufficiency, as pointed out e. g. by [1]. Stability is also affected if $\alpha h^2/\nu$ becomes large. This ratio is termed as (second) Damköhler number. By increasing mesh size, the magnitude of the Péclet and the Damköhler numbers increases and eventually a root undergoes a sign change.

In the non-linear case, identification of distinct Jacobian terms enables the mesh Péclet and Damköhler numbers to quantify the ratio between total Jacobian-convection Γ_i or the total Jacobian-reaction A against the total Jacobian-diffusion N_{ij}.

$$\Gamma_i = \beta_i + \mathring{\beta}_i - (\gamma_i + \mathring{\gamma}_i) \tag{35}$$

$$A = \alpha + \mathring{\alpha} \tag{36}$$

$$N_{ij} = \nu_{ij} + \mathring{\nu}_{ij} \tag{37}$$

Since Γ_i is a vector, A a scalar and N_{ij} a tensor, $N_{ij}^{-1}\Gamma_i$ is the vector pointing in the streamline direction. By defining the mesh size to be aligned with the streamline vector, following distinct indicators are constructed for multi-dimensional elements based on inner and outer products:

$$\text{Péclet number} \quad Pe = h_j N_{ij}^{-1}\Gamma_i \tag{38}$$

$$\text{Damköhler number} \quad Da = h_j N_{ij}^{-1} h_i A \tag{39}$$

In a broader sense, condition (34) needs to be fulfilled to obtain a consistent solution. Therefore, condition (34) now reads

$$3|Pe| + Da < 6$$

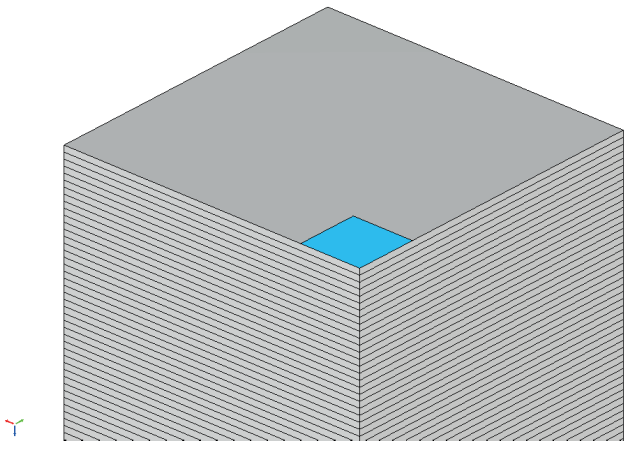

Fig. 1. The sensor has symmetry which allows to simulate a quarter of the whole model.

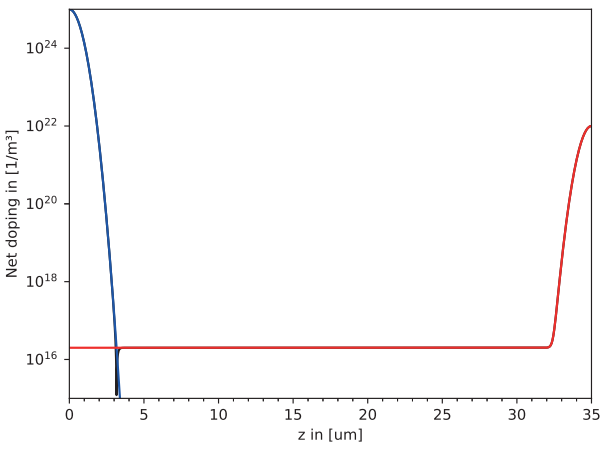

Fig. 2. The doping concentration levels in the diode. Red line shows the negative background doping N_{D}, blue line shows the positive doping N_{A}

and needs to be fulfilled to obtain a consistent solution. If the condition is not fulfilled, we expect the solution to exhibit spurious oscillations and thereby the Newton iteration to stagnate or diverge. There are two simpler conditions which are derived for the convection dominated $|Pe| < 2$ and the reaction dominated $Da < 6$ cases.

The generalization of the above consideration to the multi-dimensional and multi-physical cases is ambiguous. Even the correct quantification of h is debatable. It is common to either take the diameter of the element, the longest edge or the extend in the direction of convective flow (streamline direction). Progress to generalize to the multi-physical case are scarce e. g. [12]. In this case the positive root criterion has to be replaced by a corresponding condition of positivity of the eigenvalues of the system of differential equations. However, simple criteria like (34) so are not available in the general case.

V. Numerical example

Provided with explanations above, we now apply the Péclet and Damköhler numbers for indication of solution inconsistencies to the semiconductor problem. To apply the instability indication to the practical example of the semiconductor drift-diffusion problem, we examine the simulation of a pn-diode as shown in Fig. 1.

A. Geometry

The diode geometry is an elongated cuboid in the z-direction that is symmetrical along the x-z as well as y-z planes. An advantage of the symmetry is taken by reducing the model to a quarter cut-out and adjusting the boundary conditions accordingly. The continuity at the symmetry planes is modeled by an electrically isolating boundary condition since it may be assumed that any currents in the normal directions to the planes would vanish.

The model side lengths in the quarter model measure $d_{x,y} = 10\,\mu$m, the depth in the z-direction is $d_z = 35\,\mu$m. The discretization in the z-direction h_z has been chosen smaller than $h_{x,y}$ in the cross-sectional directions. The surface of the biasing contact has been meshed by triangular elements of size $h_{x,y} = 0.1\,\mu$m. The default setup features the mesh size in the z-direction (direction of diode depth) equal to $h_z = 0.1\,\mu$m whereas the cross-sectional discretization mesh size was set to $h_{x,y} = 1\,\mu$m. To investigate the effect of mesh size on the solution process, mesh size h_z has exclusively been varied while $h_{x,y}$ has been held constant during all simulations.

A negative biasing at the p-contact switches the diode into a cut-off regime. The diode operates in a high-ohmic state with elevated electrical fields and near-zero currents. A contact pad is located on one side of the diode which is connected to the biasing voltage $V_{\text{bias}} = -0.5\,\text{V}$. The biasing is applied to the p-region connector of the diode. The opposite side of the diode is contacted and kept steady at the ground reference voltage $V_{\text{g}} = 0\,\text{V}$.

The doping varies solely in the z-direction with a diffusion depth of $\sigma = 0.5\,\mu$m. The doping profile of the diode is given by

$$N_{\text{D}} = N_{\text{D}_0}\left(1 + e^{-\left(\frac{\sqrt{2}(z-35\mu\text{m})}{4\sigma}\right)^2}\right) \tag{40}$$

$$N_{\text{A}} = N_{\text{A}_0} e^{-\left(\frac{\sqrt{2}z}{4\sigma}\right)^2} \tag{41}$$

As can be seen from equations (40) and (41), the doping profile consists of a basic negative donator doping N_{D} and an additional heavy acceptor doping N_{A}. The full doping profile is depicted in Fig. 2 where the blue line indicates the donator doping concentration and the blue line shows the acceptor doping concentration.

B. Simulation Strategy

The diode geometry spatially resembles a pseudo one-dimensional problem. Except in a region near to the pad, the variation of computed quantities is assumed negligible in x- and y-directions compared to the variation in the z-direction. We

Table IV. Simulation Results

Index of setup	**Mesh size** h_z $[0.2\mu\text{m}]$	**Carrier lifetimes** $\tau_{\text{n,p}}$	**Iterations in total**	**Intermediate biasing steps**	**Iteration relaxations**	**Péclet number (max)**	**Damköhler number (max)**
1	0.2	$\tau_{\text{n}} = 3.95 \cdot 10^{-5}$	20	1	0	1.37 (n,p)	0.074 (n)
		$\tau_{\text{p}} = 3.52 \cdot 10^{-6}$					2.73 (p)
2	0.2	$\tau_{\text{n}} = 3.95 \cdot 10^{-7}$	43	2	1	1.37 (n,p)	24.4 (n)
		$\tau_{\text{p}} = 3.52 \cdot 10^{-8}$					824 (p)
3	0.1	$\tau_{\text{n}} = 3.95 \cdot 10^{-4}$	31	3	1	0.69 (n,p)	0.02 (n)
		$\tau_{\text{p}} = 3.52 \cdot 10^{-5}$					0.78 (p)
4	0.1	$\tau_{\text{n}} = 3.95 \cdot 10^{-5}$	37	3	1	0.69 (n,p)	0.21 (n)
		$\tau_{\text{p}} = 3.52 \cdot 10^{-6}$					7.67 (p)
5	0.1	$\tau_{\text{n}} = 3.95 \cdot 10^{-6}$	54	3	1	0.69 (n,p)	1.76 (n)
		$\tau_{\text{p}} = 3.52 \cdot 10^{-7}$					63.3 (p)
6	0.1	$\tau_{\text{n}} = 3.95 \cdot 10^{-7}$	95	3	6	0.69 (n,p)	$1.94 \cdot 10^{5}$ (n)
		$\tau_{\text{p}} = 3.52 \cdot 10^{-8}$					$6.76 \cdot 10^{6}$ (p)
7	0.1	$\tau_{\text{n}} = 3.95 \cdot 10^{-8}$	104	3	10	0.69 (n,p)	$5.5 \cdot 10^{10}$ (n)
		$\tau_{\text{p}} = 3.52 \cdot 10^{-9}$					$1.9 \cdot 10^{12}$ (p)

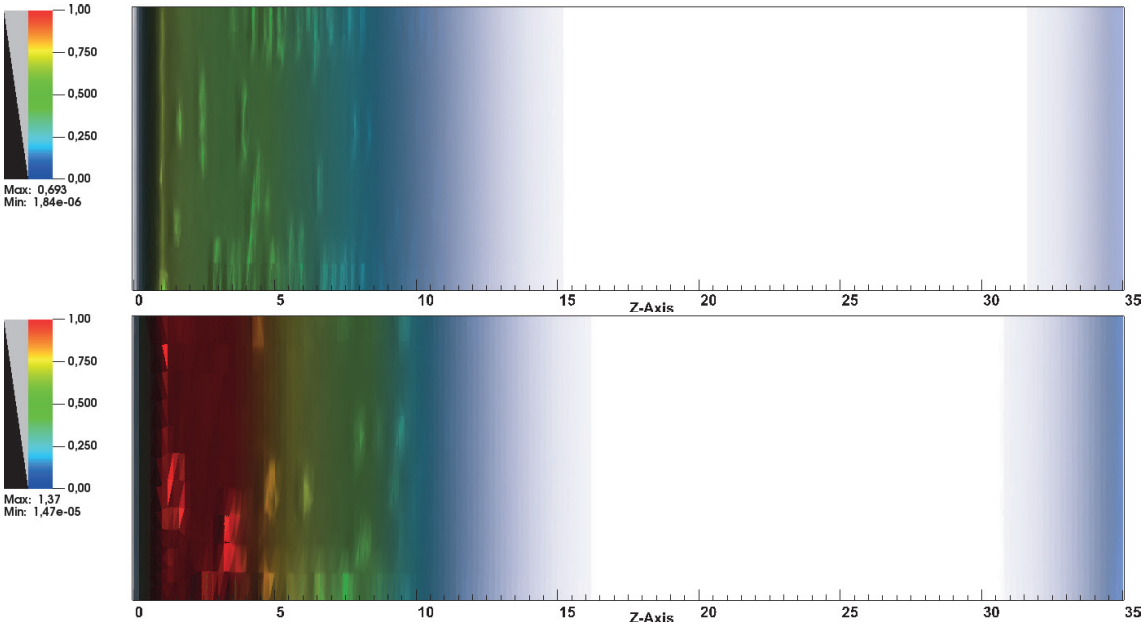

Fig. 3. Local distribution of the Péclet number for the mesh having $h_z = 0.1\ \mu$m (upper) and $h_z = 0.2\ \mu$m (lower).

make use of that arrangement by observing the instability indicators with respect to the third spatial dimension h_z.

A variation study of the mesh size h_z and of the carrier lifetimes $\tau_\mathrm{n}, \tau_\mathrm{p}$ has been carried out. Material default value used in the simulation and values of other physical parameters are provided in Table III.

For the event of iteration stagnation, the implemented Newton iteration scheme has several mechanisms to sustain solution process such as application of relaxation to the iteration update vector (down-scaling of an intermediate update) or the reduction of the biasing voltage at the clamps by a factor between zero and one. The application of these damping techniques is a deviation from a pure Newton iteration and is accounted as undesirable behavior. However, the non-linearities of the drift-diffusion model for semiconductors are in fact so strong, that both techniques are necessary to solve even the easiest of semiconductor problems.

The Péclet and the Damköhler numbers Pe and Da have been captured as post-processing data. The values have been deduced from the final state of the solution. During the Newton iteration Pe and Da vary according to the variation of the solution. That means that some intermediate solutions in the iteration process may show even higher numbers than what has been captured from the final result. Therefore an intermediate solution may cause the iteration to diverge.

VI. Simulation results

The examination of the solution stability is done by observation of the Péclet number, the Damköhler number and the iteration procedure. Stagnating iteration is quantified by a combination of several measurements: The number of total iteration count, the number of intermediate biasing steps and the number of uses of relaxation during the whole iteration. Table IV provides an overview of simulated setups and obtained results.

From analysis of the solution studies presented in Table IV the main finding is that the Péclet number and the Damköhler number correlate well with the iteration stability.

Another finding is that for the here analyzed drift-diffusion problem, the two instability indicators are rather weakly correlated with each other. It is instead observed that the Péclet number is mainly dominated by the mesh size whereas the Damköhler number, although affected by the mesh size, is mainly dominated by the electron and holes recombination time parameter.

The two correlations may be understood when (38) and (39) are evaluated by means of the coefficients of the semiconductor drift-diffusion problem. In that case, the Péclet number results in

$$Pe = \frac{h_z|\Gamma_i|}{N} = \frac{h_z\mu_{\mathrm{n,p}}|-\nabla\Psi|}{D_{\mathrm{n,p}}} = h_z\frac{|-\nabla\Psi|}{V_\mathrm{th}} \tag{42}$$

$$Da = h_z^2\frac{\frac{\partial R_\mathrm{SRH}}{\partial n,p}}{D_{\mathrm{n,p}}} \tag{43}$$

As is observed, when applied to the drift-diffusion finite-elements semiconductor formulation, the Péclet number takes on the same value for electrons or holes. It solely depends on the gradient of the electric potential and the mesh size. The Damköhler number shows a more complex behavior. It is greatly dependent on the carrier concentrations, the carrier lifetimes and the mobilities of the two carrier types.

Since both indicators may be locally evaluated on the element basis, the following presents the local distributions of Pe and Da over the mesh for the various cases mentioned in Table IV.

The highest gradients mainly form in the vicinity of the contacts and at regions of pn-junction. As can be observed in Fig. 3 an increase of mesh size from $h_z = 0.1\ \mu$m to $h_z = 0.2\ \mu$m results in a rise of the Péclet number above the tolerable threshold. By experience, these locations in the models are known to produce solution instabilities and therefore are accounted for by the users of finite-element solvers. The refinement of the mesh at these regions is therefore quite intuitive.

The sharp rise of the Damköhler number as a function of carrier lifetime may not be obvious at the first glance. The derivative of the recombination term contributes a highly non-linear term that is dependent on the local carrier concentrations of electrons and holes, the carrier lifetimes and on the mobility (which may also be a function of the electrical field). From (43) and the numerical computations it can be deducted that the recombination terms may have a great impact on the stability of the Newton iteration for the semiconductor problem. Furthermore, by means

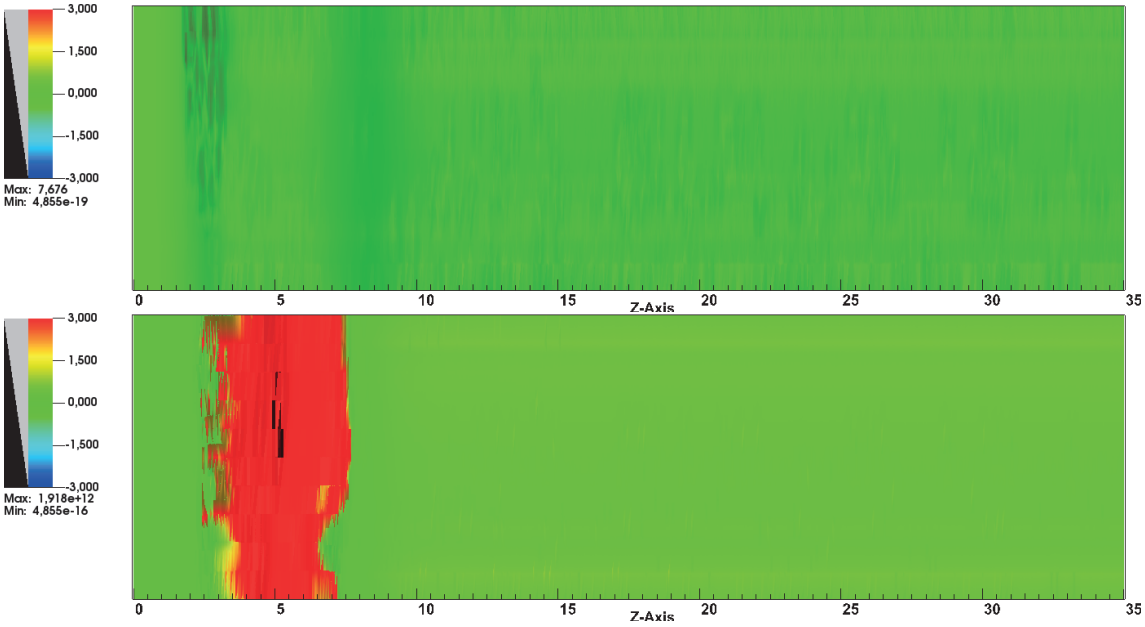

Fig. 4. Plots of the occurrence of a region with a high Damköhler number related to setup 4 and 7 in Table IV.

of indication of the Damköhler number, locations of the areas of concern may be identified as can be seen in Fig. 4. As expected, the rise of the Damköhler number is accompanied by a noticeable stagnation of the Newton iteration that can be deduced from Table IV.

References

[1] A. Quarteroni and A. Valli, *Numerical Approximation of Partial Differential Equations*. [S]pringer, 1994.

[2] H. Hernández, T. J. Massart, R. H. J. Peerlings, and M. G. D. Geers, "A stabilization technique for coupled convection-diffusion-reaction equations," *International Journal for Numerical Methods in Engineering*, vol. 116, no. 1, pp. 43–65, 2018.

[3] A. N. Brooks and T. J. Hughes, "Streamline upwind/petrov-galerkin formulations for convection dominated flows with particular emphasis on the incompressible navier-stokes equations," *Computer methods in applied mechanics and engineering*, vol. 32, no. 1-3, pp. 199–259, 1982.

[4] D. L. Scharfetter and H. K. Gummel, "Large-signal analysis of a silicon read diode oscillator," *IEEE Transactions on electron devices*, vol. 16, no. 1, pp. 64–77, 1969.

[5] S. Idelsohn, N. Nigro, M. Storti, and G. Buscaglia, "A petrov-galerkin formulation for advection-reaction-diffusion problems," *Computer Methods in Applied Mechanics and Engineering*, vol. 136, no. 1-2, pp. 27–46, 1996.

[6] E. Oñate, P. Nadukandi, and J. Miquel, "Accurate fic-fem formulation for the multidimensional steady-state advection–diffusion–absorption equation," *Computer Methods in Applied Mechanics and Engineering*, vol. 327, pp. 352–368, 2017.

[7] T. Tezduyar and Y. Park, "Discontinuity-capturing finite element formulations for nonlinear convection-diffusion-reaction equations," *Computer methods in applied mechanics and engineering*, vol. 59, no. 3, pp. 307–325, 1986.

[8] H. Gummel, "A self-consistent iterative scheme for one-dimensional steady state transistor calculations," *IEEE Transactions on Electron Devices*, vol. 11, no. 10, pp. 455–465, 1964.

[9] J. Slotboom, "Iterative scheme for 1-and 2-dimensional dc-transistor simulation," *Electronics letters*, vol. 5, no. 26, pp. 677–678, 1969.

[10] S. Selberherr, *Analysis and Simulation of Semiconductor Devices*. Springer Vienna, 2012.

[11] D. Vasileska and S. M. Goodnick, "Computational electronics," *Synthesis Lectures on Computational Electromagnetics*, vol. 1, no. 1, pp. 1–216, 2006.

[12] H.-G. Roos, "Some remarks on strongly coupled systems of convection-diffusion equations in 2d," *arXiv:1502.04473*, 2015.

Authors name and affiliation

Jürgen Anatzki, Hamburg University of Technology, Institute of Microsystems Technology, D-21073 Hamburg, juergen.anatzki@numeri-hanseatica.de

Dominik Karolewski, CiS Forschungsinstitut für Mikrosensorik GmbH, D-99099 Erfurt, DKarolewski@cismst.de,

Manfred Kasper, Hamburg University of Technology, Institute of Microsystems Technology, D-21073 Hamburg, kasper@tuhh.de